Numerical Procedures and Practical Experience of Assessment of Parametric Roll of Container Carriers

Vadim Belenky, *American Bureau of Shipping*

Han-Chang Yu, *American Bureau of Shipping*

Kenneth Weems, *Science Application International Corporation*

Abstract

The paper examines several aspects related to practical assessment of parametric roll of container carriers. The numerical procedure is based on application of the Large Amplitude Motion Program (LAMP), the nonlinear potential flow code. Viscous roll damping is included from the roll decay test. The rational choice of the loading conditions is considered. Practical non-ergodicity of the response is taken into account.

The paper also examines the way to make the development of the polar diagram more efficient. Using an envelope presentation for the irregular wave may yield a way to work with parametric roll in probability rather than in time domain. A single wave group should then be considered as an elementary random event.

Keywords: *Parametric roll, Numerical simulation Polar diagram, Envelope presentation*

1. INTRODUCTION

The problem of large amplitude roll motions caused by parametric resonance, though known for quite some time, recently made its reappearance in relation to an accident with a large container carrier, (France *et al* 2003). This paper describes the development of on-board information required by the Guide on Parametric Roll (ABS, 2004).

Below is a brief literature review on the related subject.

The physical phenomenon of parametric roll was one of the focuses of the 8th International Ship Stability Workshop that was hosted by Istanbul Technical University on October 6th and 7th, 2005 in Istanbul, Turkey.

The paper by Neves and Rodríguez (2005) looking into a new mathematical model with nonlinearities defined up to the third order in terms of the heave, roll and pitch couplings is introduced in order to simulate strong roll parametric amplifications in head seas. The influence of hull stern shape is discussed. A theoretical analysis discloses some essential dynamical characteristics associated with the proposed coupled third order mathematical model.

The paper by Umeda *et al* (2005) reviews the latest developments at Osaka University and, among others, includes theoretical prediction techniques for magnitude of parametric rolling. Poincaré mapping and averaging method were then used to obtain the magnitude of parametric roll.

A paper by Ikeda *et al* (2005) describes a model test carried out to evaluate the effect of bilge keels on parametric roll in beam seas. In the considered case, the amplitude of parametric roll decreased from 25 degrees to almost zero.

A number of papers related to parametric roll were considered at the 48th SLF. The paper SLF 48/4/12 considered parametric roll in relation to the new Intact Stability Code. Several important points were made: (1)regular wave case may be more complicated due to nonlinear behavior, (2) regular wave case appears to be more severe than irregular wave case, (3) for the irregular wave case, the probability distribution is not Gaussian.Other relevant papers at SLF-48 were focused on updating of the MSC Circular 707. The paper SLF 48/4/4 contains guidelines for all types of ships, while definition of parametric roll conditions are based on $T_R \approx 2T_E$ (T_R natural period of roll, T_E encounter period of waves) while wave length is between 0.8L and 1.2LThe paper SLF 48/4/8 also suggests that the MSC Circ. 707 guidelines be made applicable to all types of ships as far as parametric roll is concerned. The paper addresses both wave pass effect and pitch coupling and recommends changing speed and heading in order to avoid the encounter period being twice the natural roll period.The papers SLF 48/4/16 and SLF 48/4/17 describe diagrams which are meant to be present on board a vessel. Parametric roll criterion is based on the frequency range 1.9 T_E < T_R <2.1 T_R .

Papers focused on parametric roll in head and following seas also were considered during the 7th International Ship Stability Workshop that was hosted by Shanghai Jao Tong University on 1¯3 November 2004 in Shanghai, China.

Spyrou (2004) examines an approximation of transient solution of a Mathieu equation to estimate how quickly parametric roll rises. The influence of restoring nonlinearity is studied and parametric roll response is found outside of the asymptotic instability zone. The probabilistic aspect includes an envelope presentation, which leads to a formula for joint probability of height of two consecutive waves above the given threshold. The Markov chain could be used to obtain the result for the entire wave group.

The paper by Bulian et al (2004) presents the preliminary results of an analytical, numerical and experimental study regarding the problem of non-ergodicity of parametric roll in longitudinal irregular long-crested waves. A series of numerical simulations is performed with 1.5-DOF model of parametrically excited roll motion. Qualitative indications given by the numerical simulations were then compared with experimental tests, showing good agreement

2. POLAR DIAGRAMS AS A FORM OF ON-BOARD INFORMATION

2.1 Format and Information Included

Polar diagrams in wave heading/speed coordinates are a convenient way to present any numerical information for on-board use (see e.g., MSC Circ. 707). Polar diagrams for parametric roll were discussed by Shin, et al, (2003, 2004) and were recommended by ABS (2004). A Generic Polar Diagram for Parametric Roll was proposed by SLF 48/4/4.
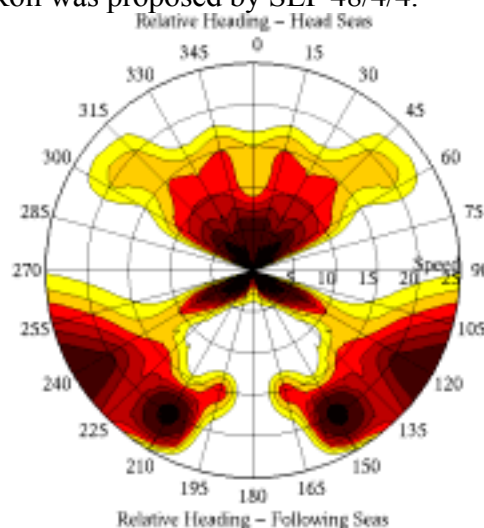

Figure 1 Sample polar diagram, Bretschnieder spectrum, with significant wave height of 12.5 m and zero-crossing period of 11.5 seconds

Polar diagrams for parametric roll considered in this paper are a further development of format (ABS, 2004). They represent the maximum roll angle observed during a one-hour simulation limited by lashing

(ABS, 1988) and engine criteria (ABS, 2006). The area of the diagram where maximum roll angle did not exceed these criteria remains black The area where these criteria were exceeded is color-coded in different types of yellow and red (from 22 to 40 degrees) in accordance with the value of observed angle. See Figure 1.

2.2   Intended Use of Polar Diagrams

These polar diagrams have been developed as a planning tool and are not intended for use when a vessel is already experiencing extreme roll motions. Real-time use of a polar diagram would be difficult. An experienced sailor is capable of evaluating significant wave height, but nearly no one could tell the exact wave heading with the naked eye. Decreased visibility and nighttime makes estimate of wave parameters even more difficult.

Most large container carriers nowadays use a weather routing service that usually includes a weather map that is updated every six hours. When a storm is on the route and a master is considering options, the polar diagrams are expected to be most useful. A weather map would include wave direction, so determining wave heading when the vessel encounters a storm will not be difficult. The speed will be also known as speed loss in waves is also known from operation experience. These two figures will determine the position of the point on the polar diagram corresponding most closely to current loading condition and expected significant wave height and zero-crossing periods of waves.

3.   DEVELOPMENT OF POLAR DIAGRAMS

3.1   Principal Numerical Tools

Parametric roll resonance is a result of changing stability in waves, so a minimum requirement for any numerical simulation tool is

a capability to compute hydrostatic forces on instantaneous submerged surface. Such software would be capable of reproducing the phenomenon, but in order to achieve numerical accuracy sufficient for practical purposes, roll damping has to match experimental results (France, et al 2003).

With computational capability currently available for mass use, application of potential hydrodynamic methods seems to be a viable, practical solution. Viscous and vortex-induced forces could be added as external components to facilitate matching of roll damping to experimental results.

Two numerical tools which meet these requirements for evaluating parametric roll are the Large Amplitude Motions Program (LAMP) and NLOAD3D codes. Both of these codes are time-domain ship motions and loads prediction codes that are built on a 3-D potential flow solution of the wave-body hydrodynamic interaction problem. Both incorporate an approximate body-nonlinear approach (Weems, et al, 2000), which computes the incident wave forcing and hydrostatic restoring pressure on the actual wetted hull surface while solving for the hydrodynamic disturbance potential on the mean wetted surface using the instantaneous ship velocity and a combined body boundary condition. This approach is sophisticated enough to capture the critical hydrodynamic phenomena associated with parametric roll while remaining fast enough to run the large number of simulations required to build the polar diagrams.

Of the two, the LAMP code is the more general implementation of the approach and suitable for multi-hull and high-speed displacement ships as well as conventional monohulls. NLOAD3D has been specifically developed for large commercial ships. Key features of NLOAD3D include an automated procedure for calibrating roll damping based on experimental roll decay data and an integrated module for setting up and running dozens of simulations over a range of speeds, headings,

and wave realizations for the polar diagram.

3.2 Environmental and Loading Conditions

Parametric roll, as with any other resonance phenomenon, is quite sensitive to excitation frequency range as well as to natural frequency of the dynamical system. Excitation frequency range is defined by a geographical region of ocean, season and other meteorological and oceanographic factors. The most precise way to present such a range is to use measured or hindcasted wave spectrum in the region of interest. Although precise, such a method is quite expensive, as the set of diagrams then becomes route-specific and unusable for other routes.

The next best way is to use approximated spectra. Most of them have two parameters related to significant wave height and mean zero-crossing period. These figures could be obtained from wave statistics-based scatter diagrams. Here, an averaged scatter diagram from IACS Recommendation 34 was used.

In order to develop set route-independent diagrams, simulations have to be performed for a series of significant wave heights and zero-crossing periods. In lieu of any other data, the simulations are performed for three most probable mean zero-crossing periods for each significant wave height. The calculations start from survival condition with 14.5 m of significant wave height and are repeated for smaller significant wave height (2 meters as a step was used in this case) until large roll motions no longer present a practical problem.

The natural roll frequency is most sensitive to *GM*, therefore, the choice of loading conditions has to cover the entire range of operational values of *GM*. In lieu of sensitivity analysis, using a smaller step for GM, where the most frequent loading conditions are, seems to be a quite practical idea.

3.3 Roll Damping Calibration

Being potential flow time-domain simulation codes, LAMP and NLOAD3D calculate only the wave component of roll damping, so the rest of the roll damping moment (vortex and friction components) has to be added. At the same time, there are no reliable methods of extracting these contributions from the result of the roll decay test. Based on previous experience (France, *et al* 2003), the best way to get a realistic simulation with respect to roll damping is to calibrate the code to produce the same results as the roll decay test.

Non-potential roll damping moment is accepted in quadratic form

$$R(\dot{\phi}) = B_1 \dot{\phi} + B_2 \, |\dot{\phi}| \, \dot{\phi} \tag{1}$$

Here, B_1 is the linear damping coefficient and B_2 is the quadratic damping coefficient.

Following the standard procedure of processing of results of the roll decay test, a straight line is fitted, using points on the roll decrement chart

$$D = k \cdot Amp + f \tag{2}$$

Here, D is a relative decrement, *Amp* is roll amplitude *Amp*), k is a slope and f is an intercept of the fitted line.

The calibration procedure for roll damping is essentially a numerical "roll decay test" being repeated for different values of damping coefficients B_1 and B_2 with the following standard roll decay processing until numerical slope and intercept would match those from the model test. This procedure could be expressed in the form of a system of two nonlinear algebraic equations and solved with any appropriate numerical method

$$(k, f) - Damp(B_1(f), B_2(k)) = 0 \qquad (3)$$

Here, *Damp* is a symbolic expression for a run of numerical simulation followed by a standard procedure of roll decay processing. Symbols $B_1(f)$ and $B_2(k)$ express that the roll linear damping coefficient depends on intercept while the quadratic roll damping coefficient depends on the slope. Practical experience has shown that the calculations converge after 5-6 iterations, on average.

3.4 Consideration of Practical Non-ergodicity and Length of Record

Practical non-ergodicity of nonlinear rolling has been addressed by a number of authors since the late 1990s (Belenky *et al*, 1997, 1998, 2001, 2003, Shin, *et al*, 2004, Bulian, *et al* 2004) and was found to be especially strong in parametric roll (Belenky 2004). The reason is that waves capable of exciting parametric roll may appear in a different sequence, one after another in one wave record or separated by "harmless" waves in another one. In the last case, kinetic energy may be dispersed before the next portion of parametric excitation will come and, as a result, the roll variance may significantly differ between records.

The practical implication of the absence of ergodicity means that several statistically independent wave records have to be used for numerical simulations. Statistical independence of wave records is achieved by using different initial phases

Another aspect to be addressed is the length of a single record. As is well known (see, for example, Belenky and Sevastianov 2003), the length of a wave record modeled by the inverse Fourier Transform is related to the frequency step. If this length is exceeded, the record can no longer be considered as statistically representative. In the case of the constant frequency step, its autocorrelation function

experiences spikes that are not related to wave physics. See Figure 2.

If the frequencies are not evenly distributed, the error still exists, but it is speeded out instead of being concentrated in the form of spikes. See Figure 3.
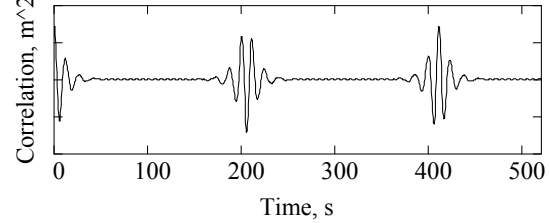

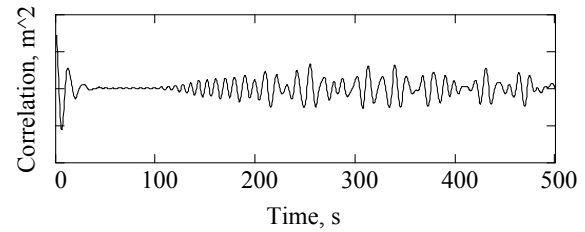Figure 2 Wave autocorrelation function for constant frequency step.

Figure 3 Wave autocorrelation function for unevenly divided frequency set.

The reason for the effect is an error in the numerical integration (Belenky 2005). The conventional inverse Fourier Transform is an equivalent of rectangular numerical integration. Respective Laplace transform allows the obtaining of the autocorrelation function directly from the spectrum:

$$R(\tau) = \int\limits_{0}^{\infty} S(\omega)\cos(\omega\tau)\,d\omega \qquad (4)$$

Here, S is spectral density, R is autocorrelation function, τ is time and ω is frequency.

It can be clearly seen that the integrand becomes quite oscillatory with time, and rectangular integration would not work well in such a case. There are integration methods that could handle oscillatory integrands[1], but their

---

[1] M. Pawlowski, 2005 Discussion at 8th International Ship Stability Workshop and private communication.

consideration is outside of the scope of this paper.

Practically, it means that the length of the wave record has to be chosen to avoid this error, and the constant frequency step has an advantage as the error-free length can be clearly defined with the following formula:

$$T = \frac{2\pi}{\Delta\omega} \qquad (5)$$

Evidently, this length could be increased by decreasing the frequency step. However, it will lead to an increasing number of wave components necessary for correct presentation of the wave spectrum. Increasing the number of wave components may lead to a significant increase in the cost of the simulation as more components have to be added up at every time step. Based on the observation, an attempt to increase the length of the simulation twice leads to a four times increase in calculation time.

At the same time, several relatively short records do have an advantage in comparison with a fewer long ones. They not only save computation time but take care of the practical non-ergodicity problem. Obviously, statistical methods should be used to estimate the accuracy that could be achieved by different combinations of number and length of records.

3.5   Some Aspects of Topology of the Polar Diagram

As the polar diagram (such as shown in Figure 1) is a result of numerical simulation, all large amplitude roll motions are included (coming from both parametric and synchronous resonance). However, a simple analysis of frequencies could reveal motions apparently coming from synchronous resonance.

One polar diagram is generated for a specific sea state defined with significant wave height and mean zero-crossing period. Each of the two-dimensional grid points of the polar diagram represent wave heading and ship speed. The encounter wave period can be determined using the mean zero-crossing period, wave heading and ship speed for each grid point. Large roll angles are often observed around the grid points where the encounter wave period is close to the roll natural period. This is typically due to the roll synchronous resonance rather than parametric roll response, which is mostly to occur near the grid points where the encounter period is one half of the roll natural period. For example, the large roll angle peaks around 20-25 knots speed near 60° and 300° headings in Figure 1 are typically due to roll synchronous resonance.

The most evident feature related to parametric roll is that, generally, the maximum angle is decreased with the increase of speed. This could be explained by the fact that roll damping increased with the speed raises the threshold of sensitivity to parametric excitation, so a lesser number of waves can transfer energy.

It is noticeable that for many such diagrams, the maximum of the parametric roll does not necessarily fall exactly in head seas. At the same time, head and following seas are expected to cause the most difference in stability between crest and trough of the wave. Shifting of maxima is also less noticeable for smaller speeds.

Such a shift of maximum can probably be explained by changes in encounter spectrum. As is well known, in head encounter, the spectrum becomes wider (see Figure 4, where four encountered spectra are shown, corresponding to 90, 120, 150, 180 degrees of wave heading).

As the encounter spectrum becomes broader, less energy is concentrated in the frequency range where the dynamical system is susceptible to parametric excitation. There are two competing factors; with 180 degrees of heading approaching, the dynamical system becomes more susceptible to parametric excitation due to increased wave influence on stability, and there

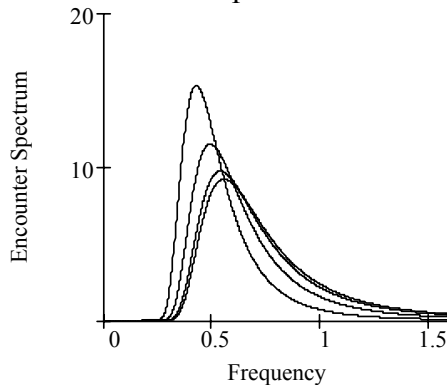is less parametric excitation due to the form of the encounter wave spectrum.

Figure 4 Transformation of encounter spectrum at 15 knots significant wave height 8.5 m

Wave direction has a smaller influence on encounter spectrum for smaller speeds; therefore, there is not as much of a shift of maximum for slower speeds.

A similar physical mechanism is responsible for topology in following seas. For the slower speeds and headings close to 90 degrees, the encounter spectrum becomes narrower, but the system already can take parametric excitation. As the concentration of energy is high (the encounter spectrum is narrow), severe parametric roll is observed. However, these conditions do not exist in the large area in the sample diagram in Figure 1 because decreasing heading and increasing speed leads to the appearance of negative encounter frequencies and even more narrow encounter spectrum. Apparently, the range of susceptible frequencies of the dynamical system is different from the frequency range of encounter spectrum, and the parametric roll mode very quickly ceases to exist.

For the cases of smaller *GM*, (see sample diagram in Figure 5), a significant area with parametric roll is also possible in following seas. Topology of such a diagram is generally similar to the one observed above and could be explained by the same physical reasons. Parametric roll in following seas is more likely because the low *GM* range of sensitivity to parametric excitation is shifted towards lower frequencies and following seas can match it.
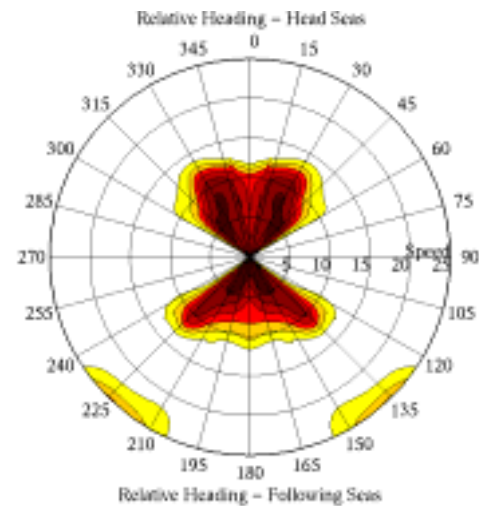

Figure 5 Polar diagram - relatively small *GM* Bretschnieder spectrum, with significant wave height of 8.5 m and zero-crossing period of 11.5 seconds

4. RISK OF PARAMETRIC ROLL

4.1 General

The principal advantage of the polar diagrams is that they can be used as an instrument of risk assessment. The problem associated with these diagrams is that their development takes a long time (weeks) to develop. This motivates the search for more efficient ways to carry out this work.

One of the possible ways to achieve better efficiency is to search for the probability of an event that roll motions caused by parametric resonance would exceed a given value. This way is also preferable as probability of exceeding would be a more representative characteristic of risk rather then maximum roll angle during one hour.

4.2 Envelope Presentation and Wave Groups: Formulation of the Problem

The envelope presentation seems to provide the natural bridge between nonlinear dynamics with periodic excitation and realistic irregular seaway. The only evident limitation of the

envelope application is how it will work for head seas when the encounter spectrum actually becomes broader. At the same time, parametric roll could be excited in a relatively narrow band of frequencies. So, it is quite possible that the narrow-band envelope presentation still may work for parametric roll in head seas despite the fact that the encounter spectrum is no longer narrow-banded. The error in this case is done to the safe side as more regular excitation leads to faster development of parametric resonance and higher roll amplitude. So, using the envelope presentation is also a conservative approach.

The envelope presentation allows presenting the seaway as a flow of wave group encounters similar to the approach taken by Tikka and Paulling (1990). Each group is to be characterized by the length of the group and the highest wave in the group. Then, the problem is to be considered in two distinct time scales:

Small time scale is the period or time duration of several minutes. It is a roll response on the group with particular characteristics and initial conditions at the "entrance" to the group. Roll autocorrelation plays a significant roll in the small time scale problem.

Large time scale is the period of quasi-stationary waves, which is the time when statistical characteristics of waves could be assumed constant. For most of practical application, it is three or six hours (the time between weather updates). The large scale problem is a random flow of independent wave groups, each of which is associated with the roll response known from the small scale problem.

4.3   Source of Data for Envelope Presentation

The envelope presentation of a stochastic process substitutes the actual process with the combination of two other stochastic processes, amplitude $A(t)$ and phase $\Phi(t)$. For the narrow-band process, it is possible to use phase shift $\varphi(t)$ and mean frequency ω_m instead of the

phase.

$$\zeta(t) = A(t)\cos(\Phi(t)) = A(t)\cos(\omega_m t + \varphi(t)) \quad (6)$$

Stochastic processes $A(t)$ and $\cos(\varphi(t))$ are slow-change figures in comparison with $\zeta(t)$, if the latter is a narrow-band process. There are a number of theoretical results available for the elements of envelope presentation, including joint distribution for $A(t)$ and $\Phi(t)$ and their derivatives as well as autocorrelation functions for $A(t)$ and $\cos(\Phi(t))$ (see a collection of these formulae in Belenky and Sevastianov, 2003).

Using these formulae, it may be possible to generate processes $A(t)$ and $\varphi(t)$ but it seems to be more practical to obtain these data directly from time history of wave elevations calculated from given spectrum in a conventional way. Calculation of amplitudes is trivial, while calculation of phase shifts requires search of times of zero-crossing Tz_j. Linear interpolation of this figure against the times when the cosine function would cross the zero yields process $\Phi(t)$; linear interpolation was also used to convert a set of amplitude points into the process. Figure 6 shows the autocorrelation function calculated from the original process plotted along with the autocorrelation function calculated from the envelope presentation. Figure 7 shows spectra calculated from the autocorrelation function with Laplace Transform. Only positive peaks were used for the calculations shown in both figures. Using negative peaks leads to similar results.

As can be seen from these figures, the proposed scheme provides a quite adequate reproduction of the original process. A more "pointy" character of the envelope spectrum could be explained by neglecting of secondary peaks, which lead to more concentration of energy around the modal frequency.
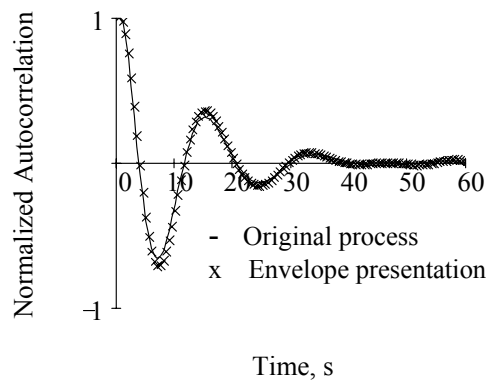
Figure 6 Autocorrelation functions for original process and envelope presentation
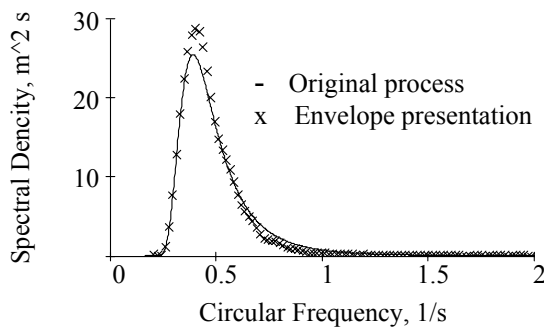

Figure 7 Spectra for original process and envelope presentation

4.4 Properties of Amplitudes and Phases

Amplitudes and phases (both Φ and φ) are stochastic processes themselves and could be characterized with respective autocorrelation functions (it is more convenient with cosine functions of phases), which are shown in Figures 8 and 9.
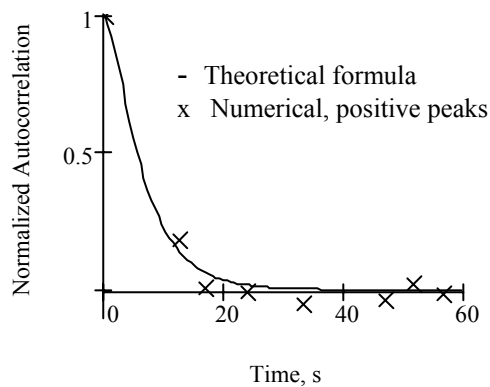

Figure 8 Autocorrelation function of amplitude

As can be seen from Figure 9, the autocorrelation function of $\cos(\Phi)$ is really close

to the autocorrelation function of the original process. It illustrates the role of phase in the envelope presentation – it keeps the memory. Autocorrelation functions of amplitude in Figure 8 and $\cos(\varphi)$ in Figure 9 show that these figures are slowly changing functions in comparison to the original process.
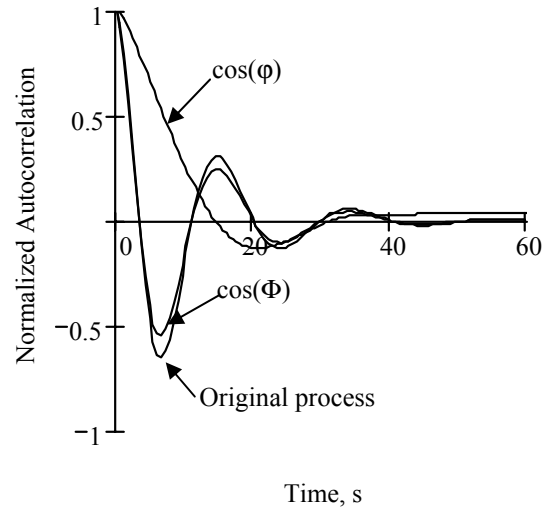

Figure 9 Autocorrelation functions original process, cosine of phase $\cos(\Phi)$ and phase shift $\cos(\varphi)$

4.5 Numerical Properties of Groups

The stochastic process of amplitudes does have its own maxima and minima. As the first expansion, the group of wave is defined as all the waves between two consecutive minima. This definition is, however, a subject for further revision, as it may lead to generation of groups that are too short.
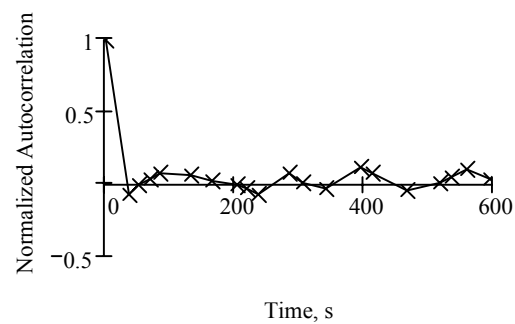

Figure 10 Autocorrelation function of group heights

Figures 10 and 11 show autocorrelation functions of group heights and lengths.

Consecutive groups could be assumed independent, as correlation drops to a small value on the second point.
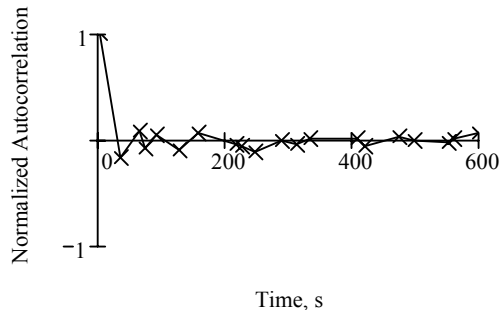

Figure 11 Autocorrelation function of group lengths

4.6   General Scheme of Numerical Assessment of Risk of Parametric Roll

Once the statistical characteristics of groups are determined by post-processing reconstructed time history of wave elevations, the entire seaway in large time scale (3-6 hours) can be presented as a flow of random events - encounters with a group.

Roll response on a group could be calculated with any appropriate numerical method, including potential codes described above. The only input to be determined for such a calculation is initial conditions, initial roll and roll rate. The initial conditions are random variables with unknown distribution (Belenky, et al 2003), so the calculations could be done for the range of initial conditions.

The values of roll angle and roll rate at the end of the group could also be called "exit conditions". The initial conditions at the beginning of the next group are identical to the exit conditions of the previous group, therefore, their distribution should be the same.

Based on the above consideration, the distribution of initial conditions could be found by the iterations, excluding the responses from the set until the distribution of the initial and exit conditions match each other with the given

accuracy. Once the iterations converge, the response set will constitute the distribution that will yield the searched probability that parametric roll would exceed the given value.

An increase of calculation efficiency may come from the ability to pre-compute the response set for the wide range of groups. The iterations procedure that is based on the statistical characteristics of the groups from the given spectrum may be faster than direct calculations. If these time savings are significant enough, it may even be used for on-board calculations. However, the final conclusions could be made only after numerical implementation and testing of the algorithm discussed above.

5.   CONCLUSIONS

The two-fold problem of parametric roll was considered here. The first part is a discussion of the polar diagram as a planning tool to prevent parametric roll.

The polar diagram is based on the maximum roll angle observed during a one-hour simulation. Criteria for polar diagrams are based on lashing strength and engine conditions. Exceeding of these criteria is color-coded, depending on the value of the roll angle. Simulations for polar diagrams are carried out using potential codes calibrated for roll damping with roll decay tests. Polar diagrams have complex topology, primarily influenced by encounter spectrum of waves and natural frequency. The choice of loading conditions should be determined by sufficient coverage of the range of natural frequency.

The second part of the paper considered application of an envelope presentation as a possible way to increase computational efficiency of the parametric roll analysis and facilitation of the application of risk evaluation methods. The proposed approach considers the problem in two-time scale, small (a wave group) and large (period while statistical characteristics

of wave are unchanged for 3-6 hrs.). Statistics for wave groups are calculated based on reconstructed seaway. Encounter with a wave group is considered as an elementary event and the problem is being solved in a probabilistic domain.

7. REFERENCES

American Bureau of Shipping, American Bureau of Shipping, 1988 "Guide for Certification of Container Securing Systems", New York

American Bureau of Shipping, 2004 "Guide for the Assessment of Parametric Roll Resonance in the Design of Container Carriers", Houston, Texas

American Bureau of Shipping, 2006 "Rules for Building and Classing Steel Vessels", Houston, Texas

Belenky, V., 2004 "On Risk Evaluation at Extreme Seas" Proc. of 7th International Ship Stability Workshop, Shanghai, China, 1-3 Nov. 2004

Belenky, V., 2005 "On Long Numerical Simulations at Extreme Seas" Proc. of 8th International Ship Stability Workshop, Istanbul, Turkey, 6-7 Oct. 2005

Belenky, V.L., Degtyarev, A.B., and Boukhanovsky, A.V., 1998, "Probabilistic Qualities of Nonlinear Stochastic Rolling," Ocean Engineering, Vol. 25, No 1, pp. 1-25.

Belenky, V.L., Suzuki, Sh. and Yamakoshi, Yu., 2001, "Preliminary Results of Experimental Validation of Practical Non-Ergodicity of Large Amplitude Rolling Motion", Proc. of 5th International Stability Workshop, Trieste, Italy, 12-13 Sept. 2001

Belenky, V. L. and Sevastianov, N.B., 2003. "Stability and safety of ships", Vol. 2 "Risk of capsizing", Elseveir, Amsterdam.

Belenky, V.L., Weems, K.M., W.M. Lin, and J.R. Paulling, 2003, "Probabilistic analysis of roll parametric resonance in head seas" Proc. of STAB'03 8th International Conference on Stability of Ships and Ocean Vehicles, Madrid, Spain

Bulian, G., Lugni, C. and A. Francescutto 2004, "A contribution on the problem of practical ergodicity of parametric roll in longitudinal long crested irregular sea", Proceedings of 7th International Ship Stability Workshop, Shanghai, China, 1-3 November

IACS Recommendation No. 34, "Standard Wave Data

Ikeda, Y., Munif, A., Katayama, A. and T. Fujiwara 2005 "Large Parametric Rolling of a Large Passenger Ship in Beam Seas and Role of Bilge Keel in Its Restraint" Proceedings of 8th International Ship Stability Workshop, Istanbul, Turkey, 6-7 Oct. 2005

France, W.M, Levadou, M, Treakle, T.W., Paulling, J. R., Michel, K. and Moore, C. 2003. "An Investigation of Head-Sea Parametric Rolling and its Influence on Container Lashing Systems," Marine Technology, Vol. 40, No. 1, pp. 1-19.

Neves M. A. and C.A. Rodríguez 2005, "Stability Analysis of Ships Undergoing Strong Roll Amplifications in Head Seas" Proc. of 8th International Ship Stability Workshop, Istanbul, Turkey, 6-7 Oct. 2005

Shin, Y.S, Belenky, V.L., Lin, W.M., Weems, K.M., Engle, A.H. 2003, "Nonlinear Time Domain Simulation Technology for Seakeeping and Wave-Load Analysis for Modern Ship Design" SNAME Transactions, Vol. 111

Shin, Y.S, Belenky, V.L., Paulling, J.R., Weems, K.M., Lin, W.M., 2004, "Criteria for Parametric Roll of Large Containerships in Longitudinal Seas", SNAME Transactions Vol. 112

SLF 48/4/4 Review of MSC/Circ.707 to include parametric rolling in head seas (Australia and Spain)

SLF 48/4/8 Proposed Revision of MSC/Circ.707 (to include parametric rolling in head seas) (Germany)

SLF 48/4/12 On the development of performance-based criteria for ship stability in longitudinal waves (Italy)

SLF 48/4/16 Proposal on MSC/Circ.707 revision (Russian Federation)

SLF 48/4/17 Proposal on MSC/Circ.707 revision (Russian Federation)

Spyrou, K.J. 2004, "Criteria for parametric rolling?", Proceedings of 7th International Ship Stability Workshop, Shanghai, China, 1-3 Nov. 2004

Tikka, K.K. and J.R. Paulling, 1990 "Prediction of Critical Wave Conditions for Extreme Vessel Response in Random Seas", Proc of. 4th International Conference on Stability of Ships and Ocean Vehicles (STAB'90), Naples, Italy

Umeda, N., Hashimoto, H., Paroka, D. and M.Hori 2005 "Recent Developments of Theoretical Prediction on Capsizes of Intact Ships in Waves", Proceedings of 8th International Ship Stability Workshop, Istanbul, Turkey, 6-7 Oct. 2005

Weems, K. M., Lin, W. M., Zhang, S., and Treakle, T., "Time Domain Prediction for Motions and Loads of Ships and Marine Structures in Large Seas Using a Mixed-Singularity Formulation," Proceedings of the Fourth Osaka Colloquium on Seakeeping Performance of Ships (OC2000), Osaka, Japan, 17-21 October, 2000.